Nature Environment and Pollution Technology
An International Quarterly Scientific Journal

p-ISSN: 0972-6268
(Print copies up to 2016)
e-ISSN: 2395-3454

Vol. 24 | No. 1 | Article ID B4228 | 2025

Original Research Paper

https://doi.org/10.46488/NEPT.2025.v24i01.B4228

Open Access Journal

Environmental Assessment Methods for Dissolution of Soil

Deepanjali Sahu[1†], M. K. Tiwari[1] and Arunachal Sahu[2]
[1]Dr. C. V. Raman University, Kota Bilaspur, C.G., India
[2]Chhattisgarh Swami Vivekanand Technical University, Bhilai, C.G., India
†Corresponding author: Deepanjali Sahu; deepanjalisahu23@gmail.com

Abbreviation: Nat. Env. & Poll. Technol.
Website: www.neptjournal.com

Received: 14-06-2024
Revised: 22-07-2024
Accepted: 23-07-2024

Key Words:

Environmental assessment
Shear stress
Cyclic resistance ratio
Cyclic stress ratio
Factor of safety
Liquefaction resistance

ABSTRACT

Water plays a crucial role in the environment and in the process of liquefaction, which can occur during moderate to major earthquakes and cause significant structural damage. Liquefaction is defined as the transformation of granular material from a solid state to a liquid state, a process driven by increased pore water pressure and reduced effective stress within the soil. When an earthquake strikes, the shaking causes the pore water pressure between the sand grains to rise, which in turn reduces the contact forces between the grains. As a result, the sand loses its effective shear strength and starts to behave more like a fluid, leading to instability and potential collapse of structures built on such ground. Liquefaction can occur in moderate to major earthquakes, resulting in severe damage to structures. The transformation of granular material from a solid state to a liquid state due to increased pore pressure and reduced effective stress is defined as liquefaction. When this happens, the sand grains lose their effective shear strength and will behave more like a fluid. This phenomenon of dissolution of soil damages trees' stability and disturbs the formation of the earth's surface. Liquefaction resistance of soil depends on the initial state of soil to the state corresponding to failure. The liquefaction resistance can be evaluated based on tests on laboratory and in situ tests. For this research, liquefaction resistance using in-field tests based on SPT N values is attempted. Cyclic resistance ratio (CRR) is found based on the corrected N value. About 16 bore logs have been selected for the factor of safety calculation. The factor of safety for soil was arrived at by taking into account of corresponding corrected SPT N values. The liquefaction hazard map is prepared for the moment magnitude of 7.5-7.6 M w. It is also found that the areas close to water bodies and streams have the factor of safety less than unity. The bore log of locations having a factor of safety less than one indicates that up to a depth of about 6 m, very loose silty sand with clay and sand is present, which are defined as medium to fine sand having low field N values.

Citation for the Paper:

Sahu, D., Tiwari, M. K. and Sahu, A., 2025. Environmental assessment methods for dissolution of soil. *Nature Environment and Pollution Technology*, 24(1), B4228. https://doi.org/10.46488/NEPT.2025.v24i01.B4228

Note: From year 2025, the journal uses Article ID instead of page numbers in citation of the published articles.

INTRODUCTION

An in-situ dynamic penetration test called the standard penetration test (SPT) is used to collect information on the soil's soil mechanics characteristics. The most common subsurface soil exploration test carried out globally is this one.

The primary goal of the test is to give a general idea of the relative density of granular deposits, including sand and gravel, from which it is nearly difficult to get undisturbed samples. The test's simplicity and low cost are its greatest strengths and the key factors behind its mass acceptance. The soil strength parameters that can be determined are approximate, but they may serve as a valuable reference in ground conditions, including gravels, sands, silts, clay that contains sand or gravel, and weak rock where it may not be practical to get borehole samples of appropriate quality.

Only soils that have filled in voids between grains of sand are liquefied. These soils are called water-saturated soils. The pressure that the water applies to the particles affects how tightly they are packed together. Before an earthquake, the pressure of water is low and stable. Yet, the water pressure may rise significantly

during the dynamic shaking, allowing the particles to freely pass one another. As that occurs, the soil deteriorates and becomes a slick, sticky liquid.

Recent geologic layers and sandy soils are the most susceptible to liquefaction in thorough field research (Fig. 1). They have also offered a database from which significant connections with engineering practices have been generated. They've demonstrated, for instance, that deposits that liquefy after one earthquake might do so once more during future ones.

Due to sandy soils, this type of liquefaction is called boiling of sand. Generally safe results of this liquefaction are "sand boils," which resemble miniature mud volcanoes (Fig. 2). Sand erupts from the soil with the same force as

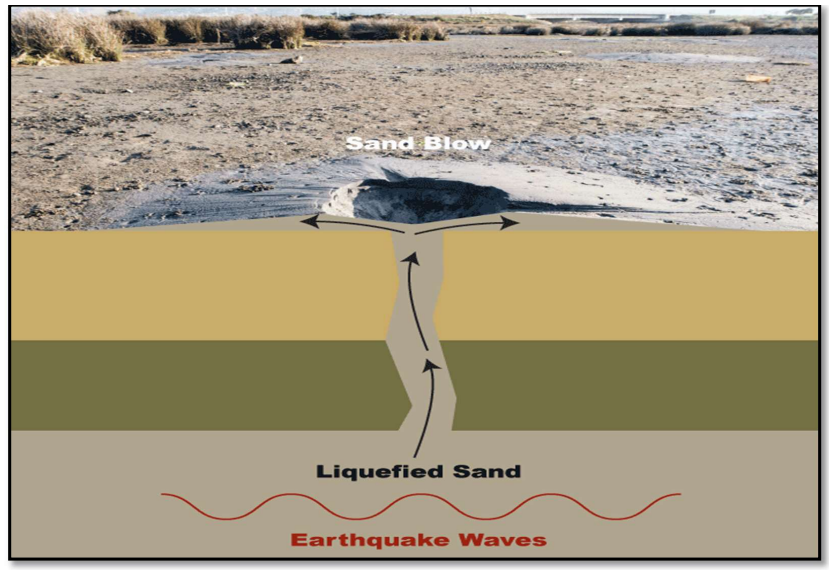

Fig. 1: Schematic vertical section showing where sills form by liquefaction during an earthquake. Reproduced from Obermeier (1996). Paleoseismic analysis of liquefaction-induced and other soft-sediment features. In: McCalpin, J.P. (Ed.), Paleoseismology. Second ed., Academic Press, Burlington, MA, pp. 497–564.

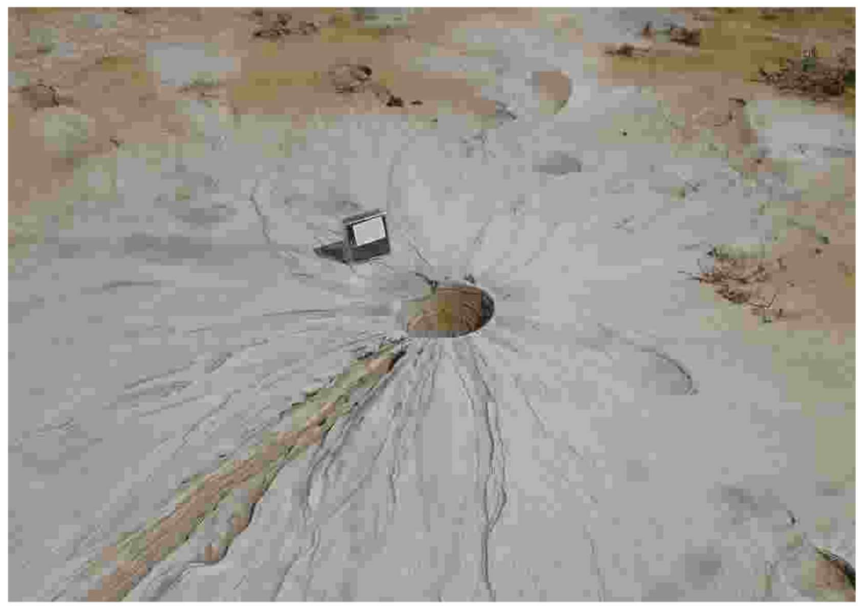

Fig. 2: One typical sand boil from Runn of Kutch's liquefied region, measuring 6 to 8 meters in diameter and 20 centimeters in height by Indian Institute of Technology, Kanpur, (https://www.iitk.ac.in/nicee/EQ_Reports/Bhuj/lique1.htm).

lava does from a volcano due to internal overpressure. A building might sink into the ground, as our feet did at the beach when soil liquefaction takes place underneath it. The structure might potentially collapse.

Some of the data used in this manuscript was obtained from an in-situ dynamic penetration test in an earthquake-affected area of Gujarat. The objective of the SPT is to determine the SPT N-value, which is an indication of the criteria governing soil strength, especially in granular soils. The SPT N-value can be correlated with soil properties for geotechnical engineering analysis and design. This value is also applicable for predicting the susceptibility of the soils to liquefaction.

A largely used liquefaction method of Standard Penetration Test (Fig. 3) of soil has been given by (Broichsitter et al. 2023, Guan et al. 2022, Zhu et al. 2021, Ordaz et al. 2023).

According to a consideration of the dynamic loading test, the cyclic pair in the cyclic load method analysis passes a high-risk zone right after it causes cyclic instability. Development-affected terrain with thick layers of soft soil and low groundwater levels is more prone to liquefaction. Results of cyclic, undrained tests on loose soils show that partially saturated soils display increased resistance at saturation levels that are only a tiny percentage below 100 (Pietruszczak et al. 2003). The triaxial tests showed how liquefaction pore pressure forms at low strains, and the fixed-base and free-top resonant column tests yielded specimens with dimensions similar to those of those tests.

The triaxial tests, which showed how liquefaction pore pressure forms at low strains, yielded specimens with dimensions similar to those of the fixed-base and free-top resonant column tests. The range of the effective stress ratios

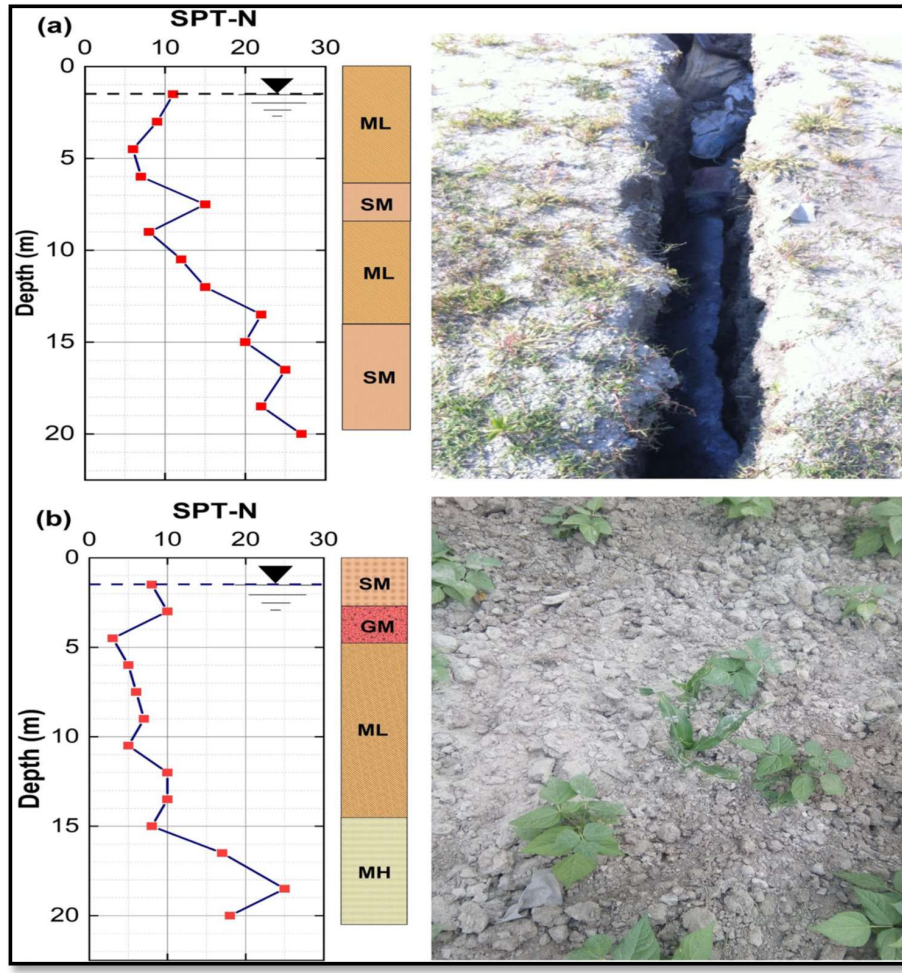

Fig. 3: Standard drill records show evidence of liquefaction in Manamaiju and Imadol during the 2015 Gorkha Earthquake (Subedi & Acharya 2022). Liquefaction hazard assessment and ground failure probability analysis in the Kathmandu Valley of Nepal, Geoenvironmental Disasters, Volume 9, Article No.: 1.

Table 1: Overview of the reviewed literature.

S. No.	Author	Methods of Analysis	Justification
1	Jethwa et al. (2018)	Deterministic In-situ analysis software	This report provides an overview of an alternative approach to assessing the liquefaction potential. The soil's back study demonstrates that there is liquefied dirt at the foundation level.
2	Liao & Whitman (1986)	Factors for Overburden Correction in SPT	Overburden factors have been analyzed over a variety of intermediate soil types, and normalizations of penetration resistance under overburden and cycle resistance ratios were performed. Overburden normalization of penetration resistances is based on either a permanent state factor or a steady void ratio.
3	Al-Jabban (2013)	Estimation of standard Penetration test (SPT)	SPT can offer dependable and practical data, the most used for geotechnical characterization tools a site mostly because of its simplicity and affordable price
4	Uprety & Lal (2021)	Standard penetration test	In this research, experiments are based on finding the N-value, or the resistance the soil presents to a sampler going inside it, which is the fundamental goal of doing SPT. Determine different soil qualities. These correlations and the field N-value help figure out the properties of the soil, but we should be aware that the tests and the empirical equations that produce the correlation have certain flaws.
5	Yusof & Zabidi (2018)	Standard penetration test (SPT) in predicting Properties of soil.	This manuscript defines test outcomes like the SPT number is significantly impacted by the shear strength parameter. Although SPT was conducted in the field on disturbed soil, it is sufficient to use SPT rather than laboratory testing to calculate the shear strength parameter. It is accurate to anticipate the shear strength parameter by taking into account the standard penetration test. The SPT number is greatly influenced by the depth of the soil, and the Atterberg limits have no impact on it because they depend on the mechanical and physical characteristics of the soil particles.
6	Skempton (1986)	Standard penetration Test with analysis of overburden	This paper analyzes soil at a given overburden pressure and constant relative density. N values might vary between various sands. By transforming the results into a conventional rod energy ratio, this impact can be completely removed. When the impacts of aging, particle size, and over-consolidation are taken into consideration, the variations that remain are fundamental to a characterization of the sands being studied and fall into a predictable pattern.
7	Gutierrez (2016)	Geostatistical data analysis of the standard penetration test (SPT)	The collection of SPT data into a single database turns out to be quite beneficial since it makes it possible to more readily spot commonalities and to combine different pieces of information for a better understanding of the soils. The usage of the geostatistics standard approach proved successful. The behavior of soils with respect to other variables that are presenting spatial variability enables us to discover potential relationships between their geomorphological traits and properties.
8	Yimsiri (2005)	Energy ratio of SPT practice	The impacts of friction, friction losses, parasitic effects of the borehole, and rod type have been analyzed for liquefaction.
9	Aggour and Radding (2001)	Standard penetration Test (SPT) correction	Different types of hammers, drill rigs, drill rod lengths, drill rod types, hammer blow rates, energy delivery systems with varying degrees of effectiveness, multiple borehole fluids, and various sampling tubes are used to measure the standard penetration resistance.
10	Kumar et al. (2016)	SPT using random number generation	In this paper, as a result, two distinct connections for cohesiveness are proposed for essentially two types of soils. Even though there are typical values for soil in the case of the angle of friction, a dramatic change in the plot's characteristics of randomly produced data is seen. Two distinct relationships for the friction angle are presented for various ranges of SPT N value as a result of this abrupt change in the plot. There are four distinct, discontinuous ranges of usual values for both the shear wave velocity and the Poisson's ratio.
11	Wazoh & Mallo (2014)	Standard penetration test	The N-value, which is essentially the resistance provided by the soil to the sampler entering inside it, is what SPT is measuring. Together with the N-value, SPT also gives us access to an SPT sample (Undisturbed Sample), which can be examined in a lab to ascertain different soil parameters. The usage of SPT is not limited to just determining N-value because it can be associated with many other soil parameters to aid in understanding the soil at the site. These correlations and the field N-value help figure out the properties of the soil, but we should be aware that the tests and the empirical equations that produce the correlation have certain flaws.

that lead to instability was shown to highlight the degree of uncertainty in that specific region.

Table 1 presents a summary of the reviewed literature on soil liquefaction analysis, outlining different methods and their justifications. Jethwa et al. (2018) employed deterministic in-situ analysis software to evaluate liquefaction potential, revealing the presence of liquefied soil at the foundation level. Liao & Whitman (1986) investigated overburden correction factors in the Standard Penetration Test (SPT), focusing on the normalization of penetration resistance. Al-Jabban (2013) highlighted SPT as a widely used, reliable, and cost-effective tool for geotechnical site characterization. Uprety & Lal (2021) conducted experiments to determine N-values, correlating them with soil properties while acknowledging the limitations of empirical correlations. These studies contribute to the broader understanding of seismic soil behavior, as discussed in prior research by (Agea et al. 2021), (Ahmadi 2015), (Ahmed et al. 2014), (Baki et al. 2012), (Bhattacharya et al. 2011), and (Bolton et al. 1985).

Positioning of Studies in Terms of Theory

Liquefaction is the loss of strength in saturated and cohesionless soils due to increasing pore water pressures and reduced effective stresses caused by dynamic loading. It is a process in which earthquake shaking (seismic effect) or other quick loading reduces soil's strength and rigid properties.

Past Records of Liquefaction

It is important to assess the possibility of seismic hazard given the recent industrial expansion in Kutch-Gujarat, especially in the largest growing regions like Mundra, Kutch, and Bhuj. The worst earthquake to hit Kutch occurred in 2001. Also, we have seen an upsurge in seismic activity in recent months. So, the crucial requirement to reduce liquefaction is the assessment of liquefaction and the appropriate selection of foundation.

The liquefaction phenomenon is one of the main findings of an earthquake's secondary effects. The liquefaction caused by the 2001 Bhuj earthquake resulted in catastrophic failures in the form of lateral spreading, sudden settlements, etc. It is necessary to comprehend the causes and modes of these failures as well as the calculation of the factor of safety, total liquefaction potential, and cumulative settlement before planning and researching mitigation strategies for such failures.

To comprehend different failure kinds and reasons, this study has examined many events, including the following-

- Bhuj Earthquake (Mag. M_w =7.7) 2001
- Kutch Earthquake (Mag. M_w = 7.5) 2001

Seismic Liquefaction Hazard in Kathmandu and Nepal

Kathmandu Valley is highly susceptible to seismic liquefaction due to its alluvial deposits, loose sandy soils, and high groundwater levels. Studies, including (KC et al. 2020) and (Pokhrel et al. 2022), confirm moderate to high liquefaction risks, exacerbated by strong seismic activity like the 2015 Gorkha earthquake (Okamura et al. 2015). Liquefaction causes differential settlement, foundation failures, and building collapses, as observed by (Sharma et al. 2016) and (Setiawan et al. 2017). Critical infrastructure, including roads and pipelines, also suffer significant damage, disrupting lifeline services.

Probabilistic models, such as those by (Sianko et al. 2020), aid in assessing earthquake hazards and mitigating risks. To reduce vulnerability, enhanced building codes, soil stabilization, and hazard-resistant planning are essential. Future research should focus on site-specific ground improvement techniques to enhance resilience against liquefaction hazards in Kathmandu Valley.

Maps of Earthquake Hazard in Gujarat

The GSDMA started a study to create a Composite Hazard Risk and Security Vulnerabilities Map for the State, which would cover six natural and man-made hazards as well as the physical, social, and economic vulnerability of its citizens, assets, and economy at the taluka level. This would serve as a framework for undertaking mitigation investments and activities. The following hazards have been thoroughly studied using sophisticated computer-aided GIS models, probabilistic analysis, and thorough field studies: seismic tremor (between a 25 and 50-year return period), and crucially for Gujarat, drought over a century.

Two earthquake hazard risk maps (for 25 and 50-year return periods) were generated based on the earthquake risk event space probability information at PGA values calculated based on IS: 1893 (Part 1) 2002 classes (Fig. 4 & 5). Where PGA is Peak ground acceleration (PGA) is the maximum ground acceleration experienced at a spot during an earthquake's shaking. PGA is defined as the maximum absolute acceleration measured on an accelerogram at a location during a specific earthquake, expressed as amplitude.

Gujarat has faced several major earthquakes causing damage due to liquefaction. Notably, the Bhuj earthquake on January 26, 2001 (Mw=7.7), led to over 13,823 fatalities and widespread destruction, while another Mw=7.5 quake on the same day devastated Kutch, destroying Bhuj and critical infrastructure (Gujarat State Disaster Management Authority). Table 2 summarizes these past events, including the October 20, 2011 (Mw=5.0) Sasangir earthquake, which

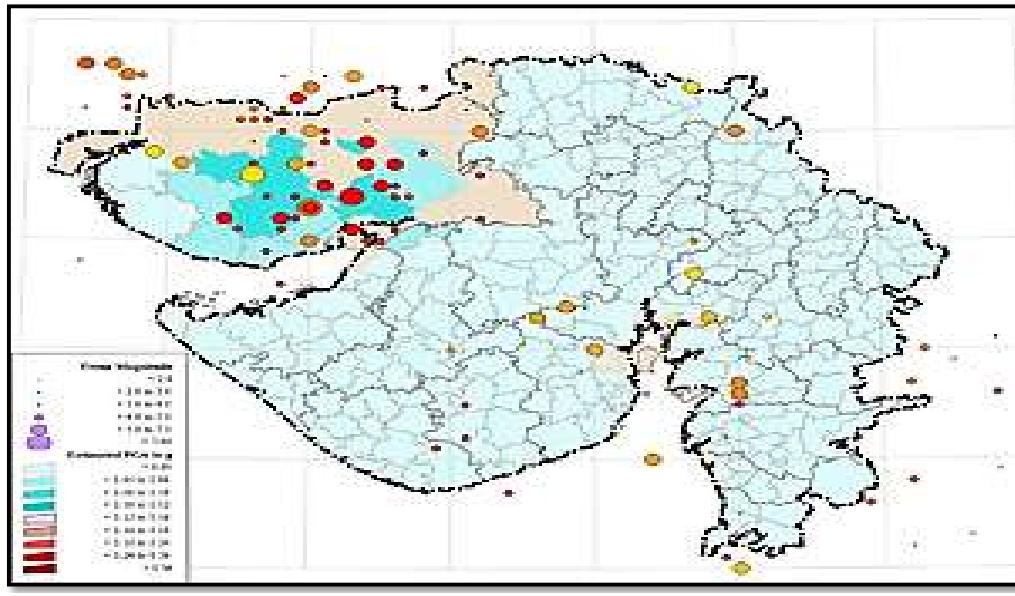

Fig. 4: The estimated mean Taluka PGA (in g) zonation for a 25-year Return period is presented [Provided by Gujarat State Disaster Management Authority, An Initiative of Government of Gujarat] assessed on dated 17/3/2024.

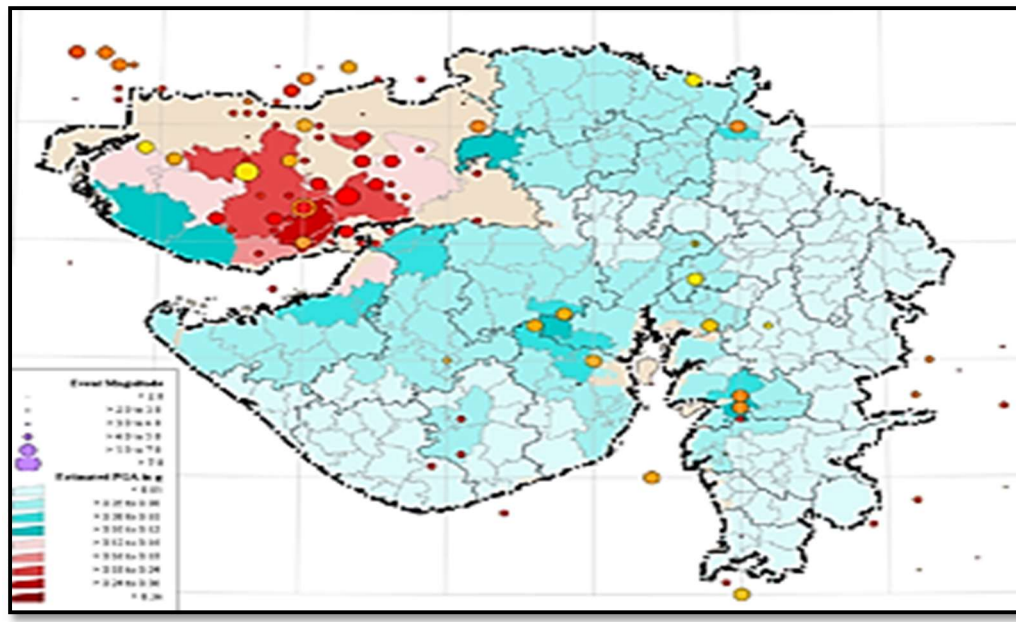

Fig. 5: The estimated mean Taluka PGA (in g) zonation for a 50-year Return period is presented [Provided by Gujarat State Disaster Management Authority, An Initiative of Government of Gujarat] assessed on dated 17/3/2024.

caused injuries and damage in Junagarh, and the August 5, 2003 (Mw=5.0) Suvi earthquake, which triggered panic across Gujarat. These incidents align with research on soil liquefaction and seismic impacts by Akin et al. (2011), (Amanta & Dasaka 2021), (Anagnostopoulos et al. 2003), (Broichsitter et al. 2023), (Chang et al. 2014), and (Chatterjee & Choudhury 2013).

MATERIALS AND METHODS

One of the in situ tests performed for coastal and near-coastal soil analysis initiatives is the Standard Penetration Test (SPT). SPT test data is often used to estimate the soil design parameters required for geotechnical analysis. However, the quality and reliability of SPT results are often unsatisfactory

Table 2: Records of events of damages in Gujarat due to liquefaction.

S. No.	Date	Place	Magnitude (Richter Scale)	Seismic Zone	Areas affected	Scale of Damage	References
1	20 Oct. 2011	Sasan Gir region, Gujarat	5.0	III	District of Junagarh, Gujarat, India	On October 20, 2011, at 22:48 local time, a mild earthquake struck the Gir National Park area of Gujarat's Saurashtra region in India. It was felt widely throughout the Kathiawar peninsula and as far away as Bombay, with a magnitude of Mw=5.0. In the district of Junagarh, there were numerous injuries and significant damage.	Gujarat State Disaster Management Authority
2	05 Aug. 2003	Suvi area, Gujarat	5.0	III	Suvi area, Gujarat, India	On August 5, 2003, at 16:38 local time, a moderate earthquake rocked Gujarat, India. It caused modest damage in eastern Kachchh and significant panic throughout Gujarat. The earthquake was Mw=5.0 in size.	National Center for Seismology Ministry of Earth Sciences, Government of India
3	26 Jan. 2001	Bhachau-Chobari (Bhuj) area, Gujarat	7.7	IV	Bhachau-Chobari, Gujarat, India	At 8:46 AM local time, a significant earthquake struck Gujarat, leaving over 13,823 people dead and significant property damage. A lower degree of damage was also sustained in the neighboring Indian states of Madhya Pradesh, Maharashtra, and Rajasthan, as well as the Pakistani province of Sindh.	Gujarat State Disaster Management Authority
4	26 Jan. 2001	Kutch, Gujarat	7.5	IV	Gujarat, Pakistan India	The price in the Kutch area was 13,000. About 20 kilometers separated the earthquake's epicenter from Bhuj, which was destroyed. In addition to four-hundredths of homes, eight colleges, two hospitals, and four kilometers of roads in Bhuj, the historic Swami Narayan Mandir, Praag Bhawan, and Aaina Mahal and forts were all severely damaged by the earthquake.	Gujarat State Disaster Management Authority
5	12 Sept. 2000	Bhavnagar area, Gujarat	3.8	III	Bhavnagar, Gujarat, India	The greatest shock in a seismic wave that started in 1999 and peaked in August 2000 left 1 person injured and a large no. of buildings destroyed. During the swarm, many more citizens fled Bhawnagar, and transportation services leaving the city were overrun by evacuees.	National Center for Seismology Ministry of Earth Sciences, Government of India
6	23 Mar. 1970	Anakleshwar-Bharuch area, Gujarat	5.4	III	Ankleshwar, Bhavnagar, Surat, and Vadodara	In Bharuch and the nearby villages, this earthquake resulted in 26 fatalities and 200 injuries. Bharuch City sustained significant damage. A 20-kilometer stretch of the ground was reported to have fissures, and considerable amounts of sand and water were released from them. Also, Anakleshwar, Bhavnagar, Surat, and Vadodara felt the tremor.	Avadh Ram, Broach (Gujarat) earthquake of March 23, 1970, Pure and Applied Geophysics

Table Cont....

S. No.	Date	Place	Magnitude (Richter Scale)	Seismic Zone	Areas affected	Scale of Damage	References
7	21 July 1956	Anjar in Kutch	6.0	IV	Bhuj, Keira, Bhachaau, Gandhi-dham and the port town of Kandla	The area, particularly in and around the Indian city of Anjar, suffered significant damage and several fatalities. The perceptible radius was 300 km2, and the largest damaged area was 2000 km2.	The Rann of Cutch Earthquake of 21 July 1956, India Meteorological Department
8	27 Nov. 1945	Makran coast, Pakistan and kachchh	8.0	IV	Makran coast, Pakistan and kachchh	At least 2,000 deaths were reported from Iran and southern Pakistan. Twelve-meter-high tsunamis hit the Makran coast. Ormara area also suffered damage. Tsunamis with heights of more than 6 meters have also been recorded in Kachchh.	S.P. Prizomwala et al. (1922), Geological footprints of the 1945 Makran tsunami from the west coast of India, Marine Geology
9	23 July, 1938	Dhandhulka-Limbdi area, Gujarat, India	6.9	IV	Vikramgad, Morbi and Rajkot	Earthquakes were felt in Vikramgad, Morbi, and Rajkot. Southwest of Ahmedabad lies this region. felt in Vikramgad, Morbi and Rajkot. The Paliyad earthquake is another name for this event.	Seismological features of the Satpura earthquake, Indian Academy of Sciences
10	15 Aug. 1906	North of Bakhasara, Rajasthan, India	6.2	IV	Rajputana, Jodhpur, Ahmedabad, India	Gujarat, Sindh, and the India-Pakistan border all heavily felt this seismic effect. Rajputana, Jodhpur, Ahmedabad, and the area around the Gulf of Khambaat also experienced it for a few seconds.	Gujarat State Disaster Management Authority
11	16 June 1819	Rann of Kachchh, Gujarat	8.2	IV	Kachchh and nearby southern Pakistan regions	In Kachchh and nearby southern Pakistani regions, several towns and villages were destroyed, and 2,000 people died. The earthquake caused significant surface deformation, including the elevation of the Allah Bund, a 90-kilometer stretch of land, by several meters.	M. G. Thakkar et al. (1912), Terrain response to the 1819 Allah Bund earthquake in western Great Rann of Kachchh, Gujarat, India, Current Science Association

for a variety of reasons, including varying hammer drop height, drive rod tilting, and erroneous hammer firing resulting in incomplete energy transfer.

Introduction of SPT (Standard Penetration Test)

This test was primarily used to correlate soil-specific gravity, but today, it is used to build foundations based on load calculations. Numerous studies have been conducted to link the SPT N value of different soil properties. Various modifications are made to the SPT N-value fields since these correlations cannot be exact.

In this area, (Kumar et al. 2006) found that there are significant fault lines near Mumbai that are close to the area of Mumbai where liquefaction was studied.

The two variables used for the liquefaction estimation or calculations, which are determined using cyclic stress techniques, are as follows:

1. Cyclic Resistance Ratio (CRR): The cyclic resistance ratio is a measure of a soil's ability to resist liquefaction. Using the information from the SPT test, the most commonly used method of calculating liquefaction resistance,
2. CSR or cyclic stress ratio: The cyclic stress ratio serves as a representation of the seismic stress on the soil layers. Liquefaction could occur during an earthquake if the cyclic stress ratio induced by the earthquake is higher than the cyclic resistance ratio of the soil in situ.

Liquefaction assessment methods include the Cone Penetration Test (CPT) and Shear Wave Velocity (Vs) techniques, as compared by (Robertson 2015), and cyclic liquefaction evaluation via CPT (Robertson & Wride 1998). The Standard Penetration Test (SPT) is another common method, though it has limitations as discussed by (Sermalai et al. 2022), and can be improved using correlations with

other metrics (Ulmer et al. 2020). Surface analysis techniques for liquefaction evaluation have been explored by Shelley et al. (2014). Mitigation strategies, such as using gravel and geosynthetics, have been studied by (Setiawan et al. 2018), while seismic spectral acceleration estimations for risk assessment were analyzed by (RaghuKanth & Iyengar 2007). Kumar & Choudhary (2016) explored engineering property estimations from SPT results. Probabilistic models, such as those by (Sianko et al. 2020), aid in assessing earthquake hazards and mitigating risks. To reduce vulnerability, enhanced building codes, soil stabilization, and hazard-resistant planning are essential.

A flowchart shown in Fig. 6 presents the Standard Penetration Test (SPT) procedure, covering key steps such as sample collection, data filtering based on distance criteria, data interpretation, statistical analysis, correlation between DPT, and comparison with literature review before concluding with result analysis. The process highlights key considerations in evaluating soil properties through SPT. This study aligns with previous research on SPT and soil liquefaction assessment, as discussed in works by (Anbazhagan et al. 2013, 2012), (Fang et al. 2023), (Ghorbani & Rajab 2020), (Bolton et al. 1985) and (Atalic et al. 2021).

Flow Chart of Standard Penetration Test

Sample Collection

A borehole must be dug to the specified sampling depth for this test. The test uses a 650mm long, heavy-walled sample

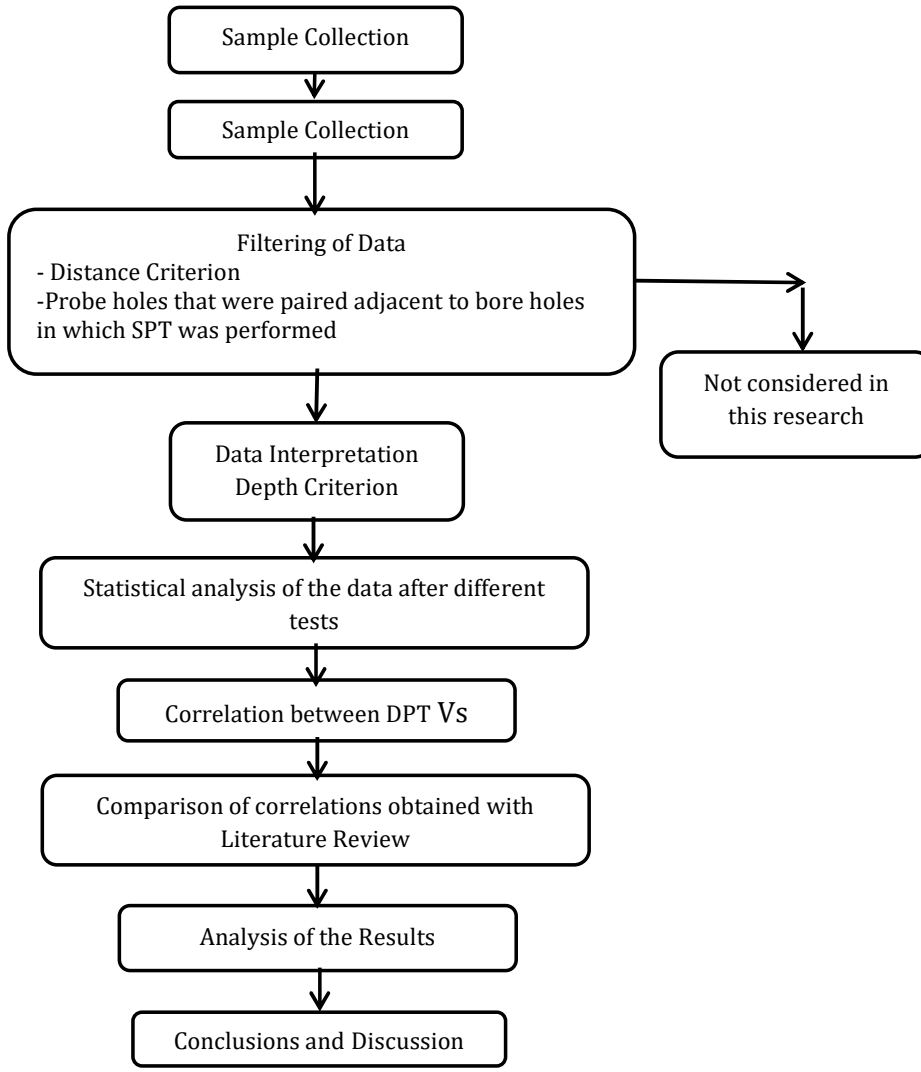

Fig. 6: Flowchart of the Standard Penetration Test (SPT) Procedure, illustrating key steps from sample collection to result analysis.

Fig. 7: The image shows the borehole location and Sample collection location by SPT at B.H. no.–1, Geomorphic features, and selected profiles in the study area, 2001 Bhuj earthquake Mw 7.5. Assessedby site of Kandla.

Fig. 8 (a)

Fig. 8 (b)

Fig. 8 (a) and (b): Photograph of the appearance of the soil sample of B.H. No. -1 (Between 3-5, 5-7, 10-12, and 12-15 m depth) of Kandla, Bhuj, Gujrat.

tube with an outer diameter of 50.8mm and an inner diameter of 35mm. The spoon sampler connected to the drill pipe is set down at the examination site.

The sampler is driven into the ground to a depth of 15 cm by continuously striking a hammer weighing 63.5 kg (140 lbs (long drill distance)) from a height of 76 cm (30 in) (6 in). It is noted how many strokes are necessary. This process is repeated two more times for a total insertion of 45 cm (18 inches).

Fig. 7 illustrates the borehole location and sample collection process using the Standard Penetration Test (SPT) at B.H. No. 1, highlighting geomorphic features and selected profiles in the study area. This location was assessed in relation to the 2001 Bhuj earthquake (Mw 7.5), specifically at the Kandla site.

Fig. 8(a) and 8(b) depict the retrieved soil samples from B.H. No. 1 at various depths (3-5 m, 5-7 m, 10-12 m, and 12-15 m) in Kandla, Bhuj, Gujarat, providing crucial insights into the subsoil characteristics of the earthquake-affected region.

RESULTS AND DISCUSSION

Data Interpretation

The usual penetration tests were carried out in accordance with the IS Code. However, the measured SPT-N value is affected by many variables, including the hammer, sampler, drilling techniques, rod types used in drilling, and hole size. All drill holes and samples shown in Fig. 6, 7, and 8 were subjected to standard penetration testing to 7m by 150mm diameter. For a geotechnical investigation, soil samples were taken from both damaged and undisturbed areas during drilling. At shallow depths, STP-N values are often low. However, there are more punches at deeper levels. No strike counts greater than 50 were observed, even at depths of 67 m, indicating liquefied behavior in the shallow layer of the study area. The estimated CRR is used to correct the SPT-N values.

Table 3 outlines the borehole data and soil classification for the study area, providing Standard Penetration Test (SPT) values and soil types at varying depths across locations including Bhuj, Mundra, Kutch, and Kandla. This data is essential for understanding the soil composition and its resistance characteristics, which are critical in evaluating the potential for soil liquefaction in earthquake-prone areas. In Bhuj, the soil predominantly consists of silty sand and coarse sand, with SPT values increasing from 5 (at 3-5 m) to 15 (at 13-15 m), indicating a shift from relatively loose to moderately dense conditions. Similarly, both Mundra and Kutch feature a mixture of coarse sand, silty sand, and silt, with SPT values ranging from 9 to 22, suggesting varying levels of compaction. Kandla, however, exhibits notably lower SPT values (4-6) across all depths, with soils primarily composed of silt and clay, which are more prone to deformation under seismic stress.

This analysis underscores the importance of site-specific soil characterization, as variations in soil properties

Table 3: Borehole data and type of soil of the study area.

B.H. No.	Location	Depth [m]	SPT Values (No. of blows)	Type of soil
1	Bhuj	3-5	5	Coarse sand
		5-7	9	Silty sand
		10-12	11	Silty sand and coarse sand
		13-15	15	Silty sand and coarse sand
2	Mundra	3-5	12	Coarse sand with silt
		5-7	9	Coarse sand
		10-12	13	Coarse sand with silt
		13-15	21	Silty sand
3	Kutch	3-5	12	Coarse sand with silt
		5-7	9	Coarse sand
		10-12	12	Coarse sand with silt
		13-15	22	Silty sand
4	Kandla	3-5	4	Silt and clay
		5-7	4	Silt and clay
		10-12	5	Silt and clay
		13-15	6	Silt and clay

play a crucial role in assessing seismic risks and foundation stability. Studies such as (Aude et al. 2022), (Audemard et al. 2005), (Ayele et al. 2021), (Chaulagain et al. 2016), (Chenjia et al. 2023), and (Chopra et al. 2012) have similarly emphasized the need for detailed soil analysis in earthquake-prone regions to better understand the potential for soil liquefaction and its impact on infrastructure stability.

Correlations for Fines Content and Soil Plasticity

Another change was the quantification of the fines correction to better fit the empirical data (Table 4) and support spreadsheet calculations. In the original development, (Seed et al. 1985) found that, for a given $(N_1)60$, CRR increases with increasing fines fraction. However, it is not clear whether the increase in CRR is due to greater resistance

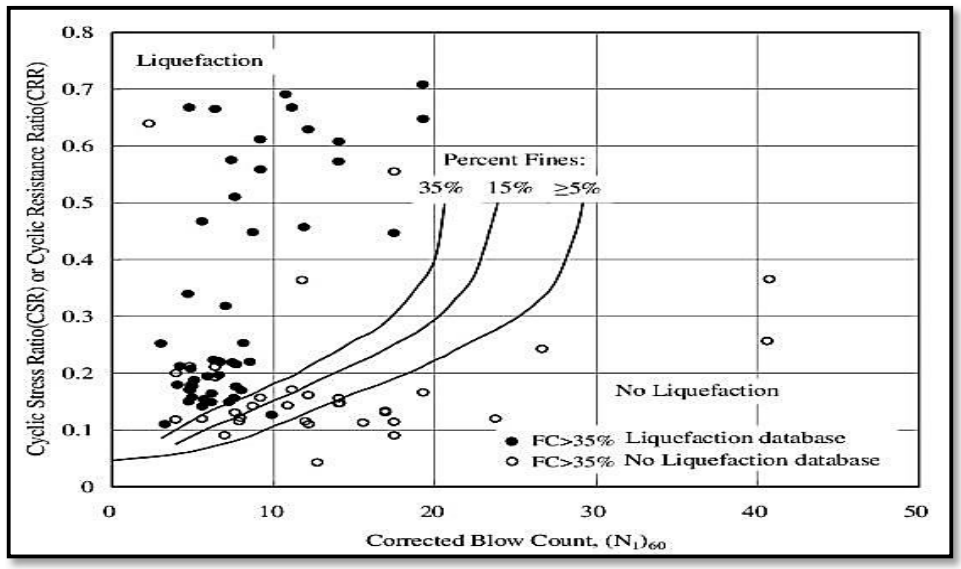

Fig. 9: Simplified baseline recommended for calculating CRR from SPT data together with empirical liquefaction data modified from (Seed et al. 1985).

Table 4: Correlation between soil sample and particle size distribution.

B.H. No.	Location	Fines Content (FC)[%]	D50 [mm]	Class of Soil	Depth of water table
1	Bhuj	4	0.50	SM	5 m
		25	0.30	SP	
		26	0.27	SP	
		26	0.27	SP	
2	Mundra	3	0.40	SP	3 m
		6	0.30	SP	
		3	0.41	SP	
		12	0.23	SM	
3	Kutch	3	0.40	SP	3 m
		6	0.30	SP	
		3	0.40	SP	
		11	0.21	SM	
4	Kandla	-	-	CH	At G.L.
		-	-	CH	
		-	-	CH	
		-	-	CH	

to liquefaction or less resistance to penetration as a result of the general increase in compressibility and decrease in permeability with increasing fines. Based on the available empirical data, Seed et al. (1985) developed CRR curves for different fines, as shown in Fig. 9.

Referring to Table 4, where, GW (Graded Gravel), GP (Poorly graded Gravel), SW (Well graded Sand), SP (Poorly graded Sand), SM (Silty Sand), GM (Silty Gravel), SC (Clayey Sand), GC are some of the different types of coarse-grained soils that are categorized (Clayey Gravel), CH (fat clays, inorganic clays with great plasticity) and D50 is the average particle diameter or mean particle size.

When the total percentage of gains reaches 50%, the appropriate particle size is D50. The term "median particle diameter" or "median particle size" is also used to refer to D50. For instance, if the D50 value for a soil sample is 5 m, this indicates that 50% of the particles are larger than 5 m and 50% are smaller than 5 m.

Due to the presence of fat clay as provided in Table 4 soil in the study area of B.H. No. 4, Kandla (Gujarat), no correlation has been found. A soil type known as "fat clays" is cohesive, elastic, and highly flexible, with a high percentage of elements that give the soil a viscous feel. When wet, difficult to deal with; when dry, strong.

Table 5 and Table 6 provide critical parameters and correlation values used in the liquefaction analysis for the study area. Table 5 outlines the key calculation parameters derived from the case study, considering an earthquake magnitude of 7.6 Mw and a peak ground acceleration (PGA) of 0.36g, based on the seismic zone classification for Kutch (Zone IV) as per IS-1893 (2002). The liquefaction potential was evaluated using the Idriss & Boulanger (2014) method, with soil sampling performed using a standard sampler in boreholes of 150mm diameter. Additionally, the lateral displacement assumptions indicate that the ground is flat across all boreholes, with no slope influence, and a 1.00m rod length was considered above ground.

Further, Table 6 presents the Cyclic Resistance Ratio (CRR) and Cyclic Stress Ratio (CSR) correlations for different borehole depths, which are essential for assessing liquefaction susceptibility. The CRR values, which indicate soil resistance against cyclic loading, vary across depths, with Borehole 1 showing a range from 0.117 at 4m to 0.165 at 9m, suggesting moderate resistance. Similarly, CSR values, representing the cyclic stress imposed by the earthquake, range from 0.215 to 0.539 in Borehole 1, highlighting variations in soil behavior at different depths. Notably, Borehole 3 exhibits a high CRR value of 0.291 at 9m, while Borehole 2 demonstrates relatively lower CRR values, suggesting different levels of soil susceptibility to liquefaction. Borehole 4 does not contain CRR and CSR data, indicating a potential lack of relevant testing or unsuitable soil conditions for analysis.

The Problem Stems from the CH Soil Type

High-plasticity clay has microscopic mineral grains that are particularly attractive to water. Although clay can usually absorb large amounts of water and still retain its strength, it expands in volume. It only takes one bad event, such as a broken water line or a major leak, for the bottom to become wet and the expansion process to begin. Once the swelling starts, it can last for years.

Table 5: Calculation parameters taken from case study.

Earthquake Magnitude	7.6 M_w
Peak ground acceleration (PGA)	0.36g (Kutch-Zone IV) (Zone factors based on Intensity of shaking IS-1893, 2002)
Calculation method	Idriss & Boulanger 2014
Sampling method	Standard Sampler
Borehole diameter	150mm
Lateral Displacement	The earth is flat for every borehole and there is no slope present.
Length of Rod	1.00m (above ground)

Table 6: Correlations for SPT using CSR and CRR.

B.H. No.	CRR				CSR			
	1 m	4 m	9 m	14 m	1 m	4 m	9 m	14 m
1	0.17	0.117	0.165	0.135	0.215	0.493	0.539	0.498
2	0.08	0.098	0.098	0.078	0.458	0.443	0.443	0.368
3	0.173	0.158	0.291	0.233	0.244	0.326	0.891	0.708
4	-	-	-		-	-	-	-

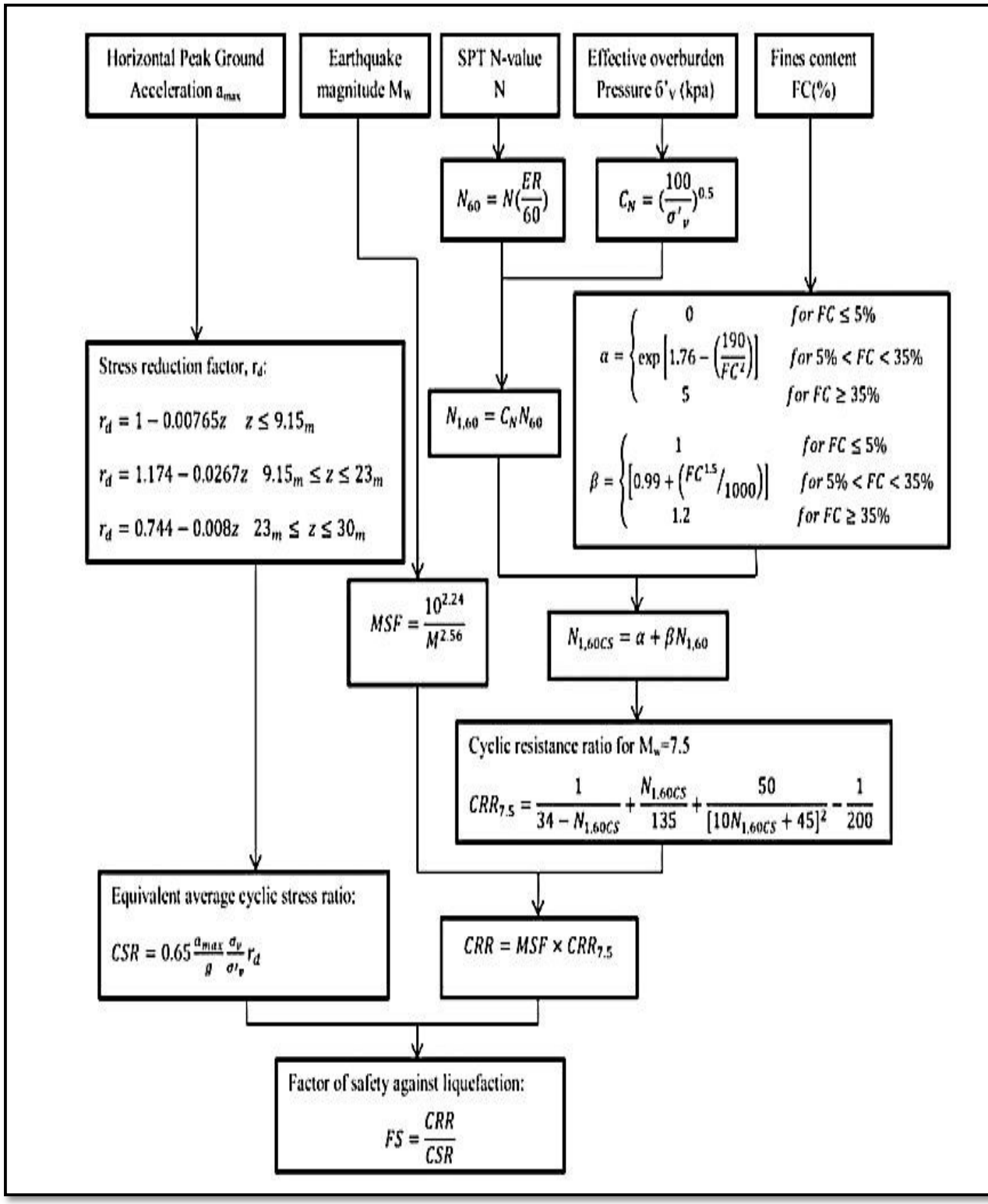

Fig. 10: Assessment of the possibility for liquefaction, using the cyclic stress method, a summary flowchart of Seed and Idriss (1971) SPT-based method with modifications in the workshops by NCEER and NSF.

Table 7: Factors of safety against liquefaction.

B.H. No.	Ration of CRR and CSR			
	1 m	4 m	9 m	14 m
1	0.79	0.24	0.31	0.27
2	0.17	0.22	0.22	0.21
3	0.71	0.48	0.33	0.33
Avg. FOS	0.6	0.3	0.3	0.3
Liquefaction Severity Index	Very Critical	Very Critical	Very Critical	Very Critical

Fig. 10 presents a systematic flowchart for calculating the Factor of Safety (FS) against liquefaction, integrating various geotechnical and seismic parameters. The process begins with the Horizontal Peak Ground Acceleration (a_max), Earthquake Magnitude (M_w), SPT N-value (N), Effective Overburden Pressure (σ›v), and Fines Content (FC%), all of which influence the soil's resistance to liquefaction.

Table 7 presents the Factors of Safety (FS) against liquefaction, determined by calculating the ratio of the Cyclic Resistance Ratio (CRR) to the Cyclic Stress Ratio (CSR) at different depths across the boreholes. The results indicate that FS values remain consistently below 1.0, highlighting a significant susceptibility to liquefaction in the study area. Borehole 2 exhibits the lowest FS values, ranging from 0.17 at 1m depth to 0.22 at 9m, suggesting extreme vulnerability to seismic-induced soil failure. Similarly, the average FS values across all boreholes at 1m, 4m, 9m, and 14m depths are 0.6, 0.3, 0.3, and 0.3, respectively, indicating that deeper layers remain highly susceptible to liquefaction. The Liquefaction Severity Index classifies all depths as "Very Critical," reinforcing the potential risk of ground deformation, excessive settlement, and structural instability during an earthquake. The findings emphasize the necessity for implementing liquefaction mitigation strategies, such as soil densification, deep foundations, or stabilization techniques, particularly in areas around Borehole 2, where the risk is most severe.

Clean Sand Base Curve

The simplified base curve's path is first changed to a low $(N_1)60$ curve with an estimated CRR intercept of roughly 0.05. With this change, the base curve is reshaped to be consistent with CRR curves.

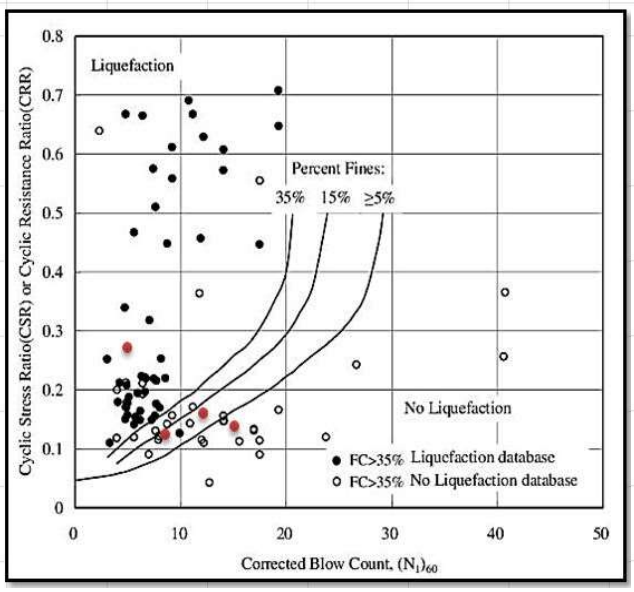

Fig. 11: Simplified Base Curve Recommended For Calculation of CRR from SPT Data along with Empirical Liquefaction Data Modified From (Seed et al. 1985) B.H.–2 mag. 7.5.

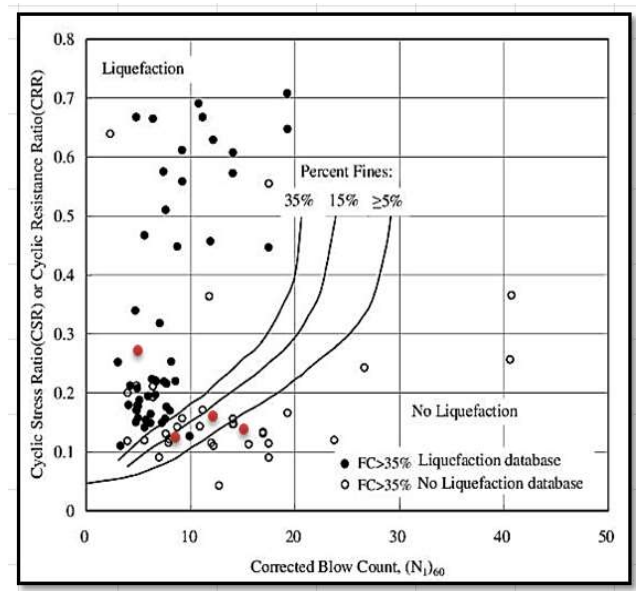

Fig. 12: Simplified Base Curve Recommended Calculation of CRR from SPT Data along with Empirical Liquefaction Data Modified From (Seed et al. 1985) B.H.–1 mag. 7.5.

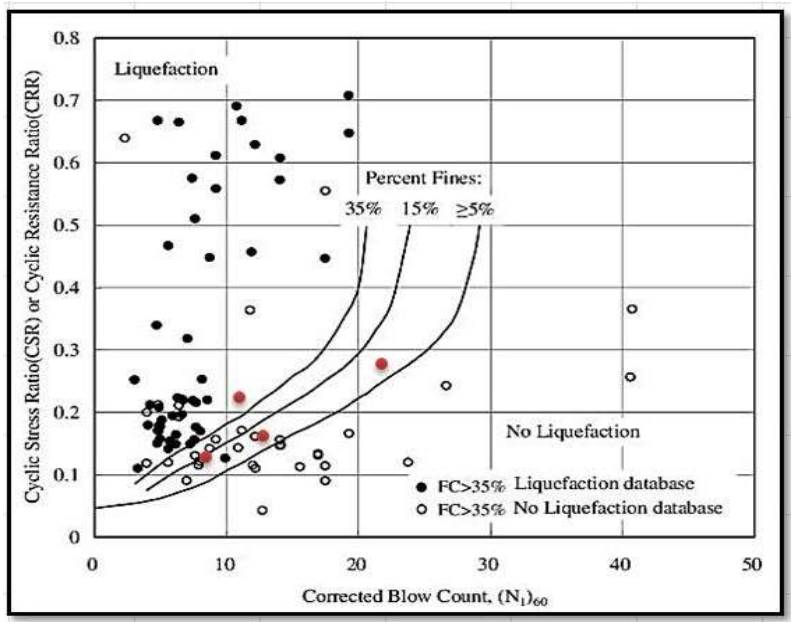

Borehole data represented by dark red color solid circle.

Fig. 13: Simplified Base Curve Recommended for Calculation of CRR from SPT Data along with Empirical Liquefaction Data modified from (Seed et al. 1985) B.H.–1 mag. 7.5.

Fig. 11, 12, and 13 illustrate the Simplified Base Curve recommended for the calculation of the Cyclic Resistance Ratio (CRR) from Standard Penetration Test (SPT) data, incorporating empirical liquefaction data modified from (Seed et al. 1985). These figures are critical in evaluating the liquefaction resistance of soil deposits, as they provide a graphical approach for estimating CRR based on SPT values under seismic loading conditions. Fig. 11 represents the base curve for Borehole 1 under a magnitude 7.5 earthquake, while Fig. 12 presents a similar base curve for Borehole 2, reinforcing the applicability of empirical correlations for liquefaction assessment. Fig. 13 further confirms the recommended base curve for Borehole 1, emphasizing the significance of SPT-based correlations in determining soil stability during earthquakes. These graphical interpretations align with previous studies, such as (Seed and Idriss 1971) and (Ishihara 1977), who developed simplified procedures to evaluate soil liquefaction potential using SPT data. Additionally, research by (Ishihara et al. 1976) and (Nath et al. 2018) has demonstrated the effectiveness of these methods in predicting liquefaction risks in various seismic regions. Ibrahim (2014) further highlighted the role of alluvial soil deposits in liquefaction behavior, which is particularly relevant for regions with loose, saturated sands. The consistency of these findings with the historical studies of (Seed et al. 1985) affirms the reliability of SPT-based empirical models in liquefaction hazard assessment. By integrating these methodologies, engineers can refine their liquefaction risk evaluation, leading to safer foundation design and improved soil stabilization techniques in earthquake-prone areas.

CONCLUSION

Using the findings of other tests for the calculation of shear wave velocity is very helpful because geophysical studies are frequently expensive and time-consuming. This work focuses on establishing and providing a link between the findings of the standard penetration test (SPT), a factor of safety (severity Index), and the shear wave velocity of soil. To achieve this, many boreholes of varying depths were dug in several liquefied areas, especially near coastal cities, and SPT was conducted there.

Concentrating on the important characteristics of soil liquefaction caused by earthquakes and evaluating areas of agreement and disagreement using the Standard Penetration Test, although it has a great focus on earthquake engineering concerns. However, there are major uncertainties in the liquefaction assessment results based on the study and experimental area. Out of four areas (Bhuj, Kutch, Mundra, and Kandla), due to the presence of fat clay soil in the study area of Kandla (Gujarat), no CSR and CRR correlation has been found. Whereas the other three areas are approaching a very critical severity index for liquefaction. Only 75% of all sites, according to liquefaction research, have a safety factor of less than one. A quarter of the sites have fat clay soil, which could reduce soil tension during an earthquake. At 1.2 meters above ground level,

a modest water table has also been observed in these areas.

After testing and analyzing various borehole soil samples from four different depths, identified the behavior of soil:

- Mostly parallel to the stream of water sources where sandy soil or muddy clay would be present, lateral spread extension has a set direction.
- The technique shows its capacity to capture the geographical distribution of liquefaction potential and quantify the liquefaction likelihood at each position of a cross-section by analyzing actual data from liquefaction from the soil of different earthquake zones.
- Technical demand parameters were also utilized to explore this method, with the aid of the soil model and its characteristics. This manuscript evaluates the effects of soil material damping on the seismic analysis of systems with soil for MDOF (multi-degree of freedom) structures.

This report provides an overview of an alternative approach to assessing the liquefaction potential. The soil's back study demonstrates that there is liquefied dirt at the foundation level up to 14 meters for all three areas, excluding Kandla; the factor of safety can be employed in this paper. It is also found that areas close to water bodies and streams have the factor of safety less than unity. The bore log of locations having a factor of safety less than one indicates that up to a depth of about 6 m, very loose silty sand with clay and sand is present, which are classified as medium to fine sand having very low field N values.

REFERENCES

Agea, A., Medina, R. and Risk, P., 2021. Risk-targeted hazard maps for Spain. *Bulletin of Earthquake Engineering*, 19, pp.5369–5389.

Aggour, M. and Radding, W., 2001. *Standard penetration test (SPT) correction*. University of Maryland, Department of Civil and Environmental Engineering; Maryland Department of Transportation, State Highway Administration.

Ahmadi, E., 2015. Importance of soil material damping in seismic responses of soil-MDOF structure systems. *Soils and Foundations*, 55(1), pp.35-44.

Ahmed, S.M., Agaiby, S.W. and Rahman, A.H., 2014. A unified CPT–SPT correlation for noncrushable and crushable cohesionless soils. *Ain Shams Engineering Journal*, 5(1), pp.63-73.

Akin, M.K., Kramer, S.L. and Topal, T., 2011. Empirical correlations of shear wave velocity (Vs) and penetration resistance (SPT-N) for different soils in an earthquake-prone area (Erbaa-Turkey). *Engineering geology*, *119*(1-2), pp.1-17.

Al-Jabban, A., 2013. Estimation of standard penetration test (SPT) of Hilla City - Iraq by using GPS coordination. *Jordan Journal of Civil Engineering*, 7(2).

Amanta, A.S. and Dasaka, S.M., 2021. Air injection method as a liquefaction countermeasure for saturated granular soils. *Transportation Geotechnics*, 30, p.100622.

Anagnostopoulos, A., Koukis, G., Sabatakis, N. and Tsiambaos, G., 2003. Empirical correlations of soil parameters based on cone penetration tests for Greek soils. *Geotechnical and Geological Engineering*, 21, pp.377–387.

Anbazhagan, P., Kumar, A. and Sitharam, T.G., 2013. Seismic site classification and correlation between standard penetration test N value and shear wave velocity for Lucknow City in Indo-Gangetic Basin. *Pure and applied geophysics*, *170*, pp.299-318.

Anbazhagan, P., Parihar, A. and Rashmi, H.N., 2012. Review of correlations between SPT-N and shear modulus: a new correlation applicable to any region. *Soil Dynamics and Earthquake Engineering*, 36, pp.52–69.

Atalic, J., Uroš, M., Novak, M.S., Demšić, M. and Nastev, M., 2021. The Mw5.4 Zagreb (Croatia) earthquake of March 22, 2020: impacts and response. *Bulletin of Earthquake Engineering*, 19, pp.3461–3489.

Aude, S.A., Mahmood, N.S., Sulaiman, S.O., Hasan Hussain Abdullah, H.H. and Ansari, N.A., 2022. Slope stability and soil liquefaction analysis of earth dams with a proposed method of geotextile reinforcement. *International Journal of Geomate*, 22(94), pp.102-112.

Audemard, F.A., Gomez, J.C., Tavera, H.J. and Orihuela, N., 2005. Soil liquefaction during the Arequipa Mw 8.4, June 23, 2001 earthquake, southern coastal Peru. *Engineering Geology*, 78(3–4), pp.237-255.

Ayele, A., Woldearegay, K. and Meten, M., 2021. A review on the multi-criteria seismic hazard analysis of Ethiopia: with implications for infrastructural development. *Geoenvironmental Disasters*, 8(1), p.1–22.

Baki, Md. A.L., Rahman, M.M. and Gnanendran, C.T., 2012. Linkage between static and cyclic liquefaction of loose sand with a range of fines contents. *Canadian Geotechnical Journal*, 49(6), pp.891–906.

Bhattacharya, S., Hyodo, M., Goda, K., Tazoh, T. and Taylor, C.A., 2011. Liquefaction of soil in the Tokyo Bay area from the 2011 Tohoku (Japan) earthquake. *Soil Dynamics and Earthquake Engineering*, 31(11), pp.1618-1628.

Bolton, S.H., Tokimatsu, K., Harder, L.F. and Chung, R.M., 1985. Influence of SPT procedures in soil liquefaction resistance evaluations. *Journal of Geotechnical Engineering*, 111(12), pp.1425–1445.

Broichsitter, S.B., Schroeder, R., Mordhorst, A., Fleige, H. and Horn, R., 2023. Soil water diffusivity as a function of the pore size distribution and pre-compression stress. *Soil and Tillage Research*, 229, p.105675.

Chang, D.W., Cheng, S.H. and Wang, Y.L., 2014. One-dimensional wave equation analyses for pile responses subjected to seismic horizontal ground motions. *Soils and Foundations*, 54(3), pp.313–328.

Chatterjee, K. and Choudhury, D., 2013. Variations in shear wave velocity and soil site class in Kolkata city using regression and sensitivity analysis. *Natural Hazards*, 69(3), pp.2057–2082.

Chaulagain, H., Rodrigues, H., Silva, V., Spacone, E. and Varum, H., 2016. Earthquake loss estimation for the Kathmandu Valley. *Bulletin of Earthquake Engineering*, 14(1), pp.59–88.

Chopra, S., Kumar, D., Rastogi, B.K., Choudhury, P. and Yadav, R.B.S., 2012. Estimation of seismic hazard in Gujarat region, India. *Natural Hazards*, 65(2), pp.1157–1178.

Fang, Y., Idriss, J. and Pirhadi, N., 2023. Neural transfer learning for soil liquefaction tests. *Computers & Geosciences*, 171, p.105282.

Ghorbani, E. and Rajab, A.M., 2020. A review on SPT-based liquefaction potential evaluation to assess the possibility of performing a risk management. *Transactions on Civil Engineering*, 27(2), pp.639-656.

Guan, Y., Liu, H., Zhang, L. and Xu, Y., 2022. Efficient three-dimensional soil liquefaction potential and reconsolidation settlement assessment from limited CPTs considering spatial variability. *Soil Dynamics and Earthquake Engineering*, 163, p.107518.

Gutierrez, L., 2016. Análise geoestatística de dados do ensaio a percussão SPT e correlações com o relevo para a cidade de Maringá-PR. *Universidade Estadual de Maringá, Centro de Tecnologia, Departamento de Engenharia Civil, Pós-Graduação em Engenharia Civil – Mestrado*.

Ibrahim, M., 2014. Liquefaction analysis of alluvial soil deposits in Bedsa southwest of Cairo. *Ain Shams Engineering Journal*, 5(3), pp.647–655.

Ishihara, K., 1977. Simple method of analysis for liquefaction of sand deposits during earthquakes. *Soils and Foundations*, 17(3), pp.1–14.

Ishihara, K., Yoshimoto, N. and Matsuo, O., 1976. Prediction of liquefaction of sand deposits during earthquake. *Soils and Foundations*, 16(1), pp.1–16.

Jethwa, A., Pandya, H. and Sharma, R., 2018. Liquefaction analysis for Kutch region using deterministic in-situ analysis software. *International Research Journal of Engineering and Technology (IRJET)*, 5(4), pp.2395–0056.

KC, A., Joshi, S., and Paudel, S., 2020. Probabilistic seismic liquefaction hazard assessment of Kathmandu Valley, Nepal. *Geomathematics and Natural Hazards Risk*, 11(1), pp.259–271.

Kumar, P., Ranjan, R., and Sharma, V., 2016. Simulation of rock subjected to underground blast using FLAC3D. *Japanese Geotechnical Society Special Publication*, 2, pp.508–511.

Kumar, R. and Choudhary, D., 2016. Estimation of engineering properties of soils from field SPT using random number generation. *INAE Letters*, 1, pp.77–84.

Kumar, S., Singh, S. and Nandini, D., 2006. Method for regulated expression of single-copy efflux pump genes in a surrogate Pseudomonas aeruginosa strain: identification of the BpeEF-OprC chloramphenicol and trimethoprim efflux pump of Burkholderia pseudomallei 1026b. *Antimicrobial Agents and Chemotherapy*, 50(10), pp. 3460–3463.

Liao, S. and Whitman, R.V., 1986. Overburden correction factors for SPT in sand. *Journal of Geotechnical Engineering*, 112(3), pp. 373–377.

Nath, S., Saha, S., Pati, P. and Sahoo, S., 2018. Earthquake induced liquefaction hazard, probability, and risk assessment in the city of Kolkata, India: Its historical perspective and deterministic scenario. *Journal of Seismology*, 22(1), pp. 35–68.

Obermeier, S.F., 1996. Use of liquefaction-induced features for paleo seismic analysis: An overview of how seismic liquefaction features can be distinguished from other features and how their regional distribution and properties of source sediment can be used to infer the location and strength of Holocene paleo-earthquakes. *Engineering Geology*, 44(1–4), pp. 1–76.

Okamura, H., Yamada, T., Matsumoto, S. and Ueda, S., 2015. Report on a reconnaissance survey of damage in Kathmandu caused by the 2015 Gorkha Nepal earthquake. *Soils and Foundations*, 55(5), pp. 1015–1029.

Ordaz, M., Yegian, M.K., Lin, L. and Giardini, D., 2023. Event-based probabilistic liquefaction hazard analysis for defining soil acceptance criteria. *Soil Dynamics and Earthquake Engineering*, 166, p. 107781.

Pietruszczak, S., Tatsuoka, F. and Zienkiewicz, O.C., 2003. Mitigation of risk of liquefaction. *Geotechnique*, 53(9), pp.833–838.

Pokhrel, R.M., Gilder, C.E., Vardanega, P.J., De Luca, F., De Risi, R., Werner, M.J. and Sextos, A., 2022. Liquefaction potential for the Kathmandu Valley, Nepal: a sensitivity study. *Bulletin of Earthquake Engineering*, *20*(1), pp.25-51.

Prizomwala, S.P., Vedpathak, C., Tandon, A., Das, A., Makwana, N. and Joshi, N., 2022. Geological footprints of the 1945 Makran tsunami from the west coast of India. *Marine Geology*, 446, p.106773.

RaghuKanth, S.T.G. and Iyengar, R.N., 2007. Estimation of seismic spectral acceleration in Peninsular India. *Journal of Earth System Science*, 116, pp. 199–214.

Robertson, P.K. and Wride, C., 1998. Evaluating cyclic liquefaction potential using the cone penetration test. *Canadian Geotechnical Journal*, 35, pp. 442–459.

Robertson, P.K., 2015. Comparing CPT and Vs liquefaction triggering methods. *Journal of Geotechnical and Geo-environmental Engineering*, 2015.

Seed, H.B. and Idriss, I.M., 1971. Simplified procedure for evaluating soil liquefaction potential. *Journal of the Soil Mechanics and Foundations Division, ASCE*, 97(SM9), pp. 1249–1273.

Seed, H.B., Idriss, I.M. and Arango, I., 1985. Influence of SPT procedure in soil liquefaction resistance evaluations. *Journal of Geotechnical Engineering, ASCE*, 111(12), pp. 1425–1445.

Sermalai, S., Mukundan, M. and Alagirisamy, S., 2022. Standard Penetration Test (SPT) pitfalls and improvements. In: Reddy, C.N.V., Muthukkumaran, K., Satyam, N., Vaidya, R., eds. *Ground Characterization and Foundations*. *Civil Engineering*, vol. 167.

Setiawan, H., Serikawa, Y., Nakamura, M., Miyajima, M. and Yoshida, M., 2017. Structural damage to houses and buildings induced by liquefaction in the 2016 Kumamoto earthquake, Japan. *Geoenviron Disasters*, 4(1), pp. 1–12.

Setiawan, H., Serikawa, Y., Sugita, W., Kawasaki, H. and Miyajima, M., 2018. Experimental study on mitigation of liquefaction-induced vertical ground displacement by using gravel and geosynthetics. *Geoenviron Disasters*, 5(1), pp. 1–9.

Sharma, K., Deng, L. and Noguez, C.C., 2016. Field investigation on the performance of building structures during the April 25, 2015, Gorkha earthquake in Nepal. *Engineering Structures*, 121, pp. 61–74.

Shelley, E.O., Mussio, V., Rodriguez, M. and Chang, A., 2014. Evaluation of soil liquefaction from surface analysis. *Geofísica Internacional*, 54(1), pp. 95–109.

Sianko, I., Ozdemir, Z., Khoshkholghi, S., Garcia, R., Hajirasouliha, I., Yazgan, U. and Pilakoutas, K., 2020. A practical probabilistic earthquake hazard analysis tool: case study Marmara region. *Bulletin of Earthquake Engineering*, 18, pp. 2523–2555.

Skempton, A.W., 1986. Standard penetration test procedures and the effect in sands of overburden pressure, relative density, particle size, aging, and over-consolidation. *Geotechnique*, 36, pp. 425–447.

Subedi, S. and Acharya, L., 2022. Liquefaction hazard assessment and ground failure probability analysis in the Kathmandu Valley of Nepal. *Geoenviron Disasters*, 9(1).

Thakkar, M.G., Ngangom, M., Thakker, P.S. and Juyal, N., 2012. Terrain response to the 1819 Allah Bund earthquake in western great rann of Kachchh, Gujarat, India. *Current Science*, pp.208-212.

Ulmer, K.J., Green, R.A. and Marek, A.R., 2020. Consistent correlation between Vs, SPT, and CPT metrics for use in liquefaction evaluation procedures. *Geo-Congress*, February 2020.

Uprety, S. and Lal, R., 2021. Standard penetration test in geotechnical engineering site investigations. *Journal of Emerging Technologies and Innovative Research*, 8(4).

Wazoh, S.A. and Mallo, S.P., 2014. Standard penetration test in engineering geological site investigations – A review. *The International Journal of Engineering and Science (IJES)*.

Yimsiri, S., 2005. Distinct element analysis of soil-pipeline interaction in sand under upward movement at deep embedment condition. In *Proceedings of the 16th International Conference on Soil Mechanics and Geotechnical Engineering*, vol. 3.

Yusof, N. and Zabidi, M.A., 2018. Reliability of using standard penetration test (SPT) in predicting properties of soil. *Journal of Physics: Conference Series*, 1082, p. 012094.

Zhu, Z., Liu, J., Yang, H. and Zhang, L., 2021. Assessment of tamping-based specimen preparation methods on static liquefaction of loose silty sand. *Soil Dynamics and Earthquake Engineering*, 143, p. 106592.